Available online at www.sciencedirect.com
SCIENCE DIRECT
Polymer 46 (2005) 4492–4503
polymer
www.elsevier.com/locate/polymer

Diffusion of water and ammonia through polyimide-silica bicontinuous nanocomposites: interactions and reactions☆

P. Musto[c], L. Mascia[a,*], G. Mensitieri[b], G. Ragosta[c]

[a]*Institute of Polymer Technology and Materials Engineering, Loughborough University, Loughborough, LE11 3TU, UK*
[b]*Department of Materials and Production Engineering, University of Naples Federico II, P.le Tecchio 80, 80125 Naples, Italy*
[c]*Institute for Chemistry and Technology of Polymers, National Research Council of Italy (ICTP-CNR), via Campi Flegrei 34, 80078 Pozzuoli, Naples, Italy*

Available online 24 March 2005

Abstract

The diffusion of low molecular weight penetrants through films of a PMDA-ODA polyimide and a corresponding polyimide-silica bicontinuous nanocomposite (organic–inorganic hybrid) was monitored using time-resolved FTIR spectroscopy and gravimetric analysis. A reacting and a non-reacting penetrant, ammonia and water vapour, were used in the study in order to evaluate their relative interactions with the components of the polyimide-silica hybrid from sorption and diffusion measurements.

In the experiments with water vapours the sorption equilibrium was measured with activity levels varying from 0.1 to 0.75. The state of water molecules was examined on the basis of a simplified H-bonding association model.

From the experiments using ammonia as the penetrant, it was possible to separate the physical diffusion component from the reaction-determined transport rate by using different sample thickness and penetrant pressure. A remarkable catalytic effect of the silica phase on the reaction of ammonia with the polyimide was observed.

Keywords: Nanocomposite; Diffusion; Polyimide

1. Introduction

Polyimides (PI) represent an important class of high-performance polymers that exhibit a very high glass transition temperature, ductility, thermal oxidative stability, and solvent resistance, coupled with relatively low permittivity and dielectric losses up to very high temperatures. For this reason these materials find applications as insulating materials in high voltage rotating machines, microelectronic devices and in separation membrane technology [1–5]. More recently, they have been used for the production of organic-inorganic (O/I) hybrids by the sol–gel route [6–10].

The sol–gel method can be viewed as a two-step network forming process, the first step being the hydrolysis of a metal alkoxide and the second consisting of a polycondensation reaction [11–15]. Polyimides are particularly suitable for the production of O/I hybrids as they can be obtained from a polyamic acid precursor, which is soluble in hygroscopic solvents and can tolerate the addition of water necessary to bring about the hydrolysis of the alkoxide. Even though the condensation reaction for the conversion of a polyamic acid to the corresponding polyimide is an intramolecular process, it has been found that the imidisation reaction is accelerated by the presence of the bicontinuous silica domains [16]. Moreover, the excellent thermal stability of polyimides allows the hybrids to be post-cured at very high temperatures (350–400 °C) making it possible the development of a very dense silica network without inducing appreciable degradation of the organic phase.

It has been demonstrated in previous investigations [5,7,10] that the morphology of these hybrid systems can be closely controlled by use of suitable coupling agents. Discontinuous, two-phase microcomposites are obtained in the absence of coupling agents, while bicontinuous nanocomposites (organic–inorganic hybrids) are obtained by introducing a functional alkoxysilane such as γ-glycidyloxypropyltrimethoxysilane (GOTMS) in the precursor solution for the formation of silica.

In a study concerned with the use internal coupling

☆Parts of this Paper were presented at The New Polymers Symposium, 23–24 October 2003, Capri, Italy

* Corresponding author.

0032-3861/$ - see front matter © 2005 Elsevier Ltd. All rights reserved.
doi:10.1016/j.polymer.2005.02.032

agents, i.e. those in which the polyimide contains pendant alkoxysilane groups in the chains, it was found that the density of the siloxane domains could be varied considerably by using different ratios of alkoxysilane to methylsilane bonds in the internal coupling sites [17]. The resulting changes the hydrophilic nature of the alkoxysilane groups affects also the final morphology of the final product [17,18].

The effect of changing the polarity within the polyimide chains on the morphology and properties of resulting O/I hybrids has been investigated very recently by using 4,4′-hexafluoroisopropylidenediphthalic anhydride (6FDA) and various types of fluorine containing diamines in the preparation of the polyimide. Internal coupling was achieved through copolymerisation with 3-aminopropyl trimethoxysilane. The refractive index of the resulting hybrids could be altered by changing the fluorine content in the polyimide chains and the silica content [19].

Although several studies have been reported on the diffusion of polyimide silica membranes [20–23] very little attention has been given to the relative interactions of penetrants with the constituents of O/I hybrids, particularly for systems where the penetrant can react with one or both components.

Diffusion through O/I membrane is greatly affected by the morphology of the inorganic domains, particularly with respect to their relative continuity, state of microclustering and the structure of the interphase [22].

Furthermore, the diffusion and sorption behaviour has been related to changes in the local chain dynamics rather than an increase in free volumes [23].

In a recent study the inorganic domains in membranes produced from polyimide-silica and polyimide-titania hybrids were found to exert a catalytic effect on the reaction of carbon dioxide with methanol to produce dimethyl carbamate [21].

The present study examines the diffusion behaviour of water and ammonia through the nanostructured bicontinuous domains of polyimide-silica hybrids. These were chosen on account of some contrasting characteristics in relation to their interactions with polyimides. Water is capable of forming microclusters in their sorption and diffusion through glassy polymers, such as polyimides [24,25].

In a related study it was indicated that the diffusion coefficient of ammonia through polyimides is much smaller than that of water, even though the van der Waals molar volume is very similar for the two penetrants [26]. This was attributed to the reactions of ammonia with the polyimide, but neither the nature of the reactions nor the kinetics of the two concurrent processes, physical diffusion and chemical reactions, were investigated in order to separate the two events. One of the objectives of the present study is to elucidate the two events related to the transport of ammonia through polyimides and polyimide-silica, as well as to illustrate the interactions of water with the respective components of the O/I hybrids examined.

In this study, information on the kinetics of diffusion and reactions were obtained through an analysis of sorption data using time-resolved FTIR spectroscopy. This offers the unique opportunity to monitor in situ the diffusion of the reagents and the chemical reaction with the two components of the O/I hybrid membrane.

2. Experimental

2.1. Materials

The polyimide precursor used in this study was Pyre-ML RK 692 from I.S.T (Indian Orchard, MA), commercially available as a 12 wt% solution in a mixture of *N*-methyl-2-pyrrolidone (NMP) and xylene (weight ratio 80/20). The precursor was a polyamic acid (PAA) formed by condensation of pyromellitic dianhydride (PMDA) and oxydianiline (ODA) having $\bar{M}_w = 1.0 \times 10^5$ and $\bar{M}_n = 4.6 \times 10^4$. High purity grades of tetraethoxysilane (TEOS) and γ-glycidyloxypropyltrimethoxysilane (GOTMS) were obtained from Aldrich (Milwaukee, WI). Distilled water was used to induce hydrolysis of the alkoxysilane components using a 32 wt% HCl solution as catalyst and ethanol as solvent.

The alkoxysilane solutions used for the production of the nanocomposite film (22.2 wt% silica) was prepared as follows:

3.46 g TEOS, 0.86 g EtOH, 1.20 g GOTMS, 082 g H_2O and 0.12 g aqueous HCl solution (2.0 wt%) were added sequentially in a glass vial. The mixture was magnetically stirred at room temperature (RT), until a clear solution was obtained. The precursor hybrid solution was subsequently prepared by adding dropwise the hydrolysed alkoxysilane solution to the polyamic acid solution, under continuous stirring for 10 min at RT.

For the production of films, the precursors solutions were cast on glass slides and kept at 80 °C for 1 h to allow most of the solvent to evaporate. Imidization and condensation reactions were carried out in successive isothermal steps of 1 h each, at 100, 150, 200, 250 and 300 °C. The achievement of full imidization of the amic acid was confirmed spectroscopically [16].

2.2. Measurements

2.2.1. Water and ammonia sorption by time-resolved FTIR spectroscopy

A vacuum tight FTIR cell was used to record the FTIR transmission spectra of the polymer films exposed to a controlled humidity environment and to dry gaseous ammonia at constant pressure. The cell was connected by service lines to different units or components, respectively, a water reservoir, an ammonia cylinder, a vacuum pump and

pressure transducers. A schematic diagram of the apparatus is shown in Fig. 1. Further details of the experimental set-up are reported elsewhere [27].

The instrument used for the collection of IR spectra was a Perkin–Elmer System 2000 spectrometer equipped with a germanium/KBr beam splitter and a wide-band DTGS detector. The instrumental parameters were as follows: resolution = 4 cm^{-1}, optical path difference (OPD) velocity = 0.2 cm/s, spectral range = 4000–400 cm^{-1}. A single data collection was performed for each spectrum (3601 data points) which took 6 s to complete under the chosen instrumental conditions. The signals were acquired as single beam spectra at specific time intervals. A typical sorption run lasted about 30 min, while the acquisition time intervals were 6 s during the first 10 min of the experiment and 60 s thereafter.

In the case of water vapour, tests were performed at 30 °C and at relative pressures, p/p_0, to obtain different activities, varying from 0.1 to 0.75 for polyimide films (20 ± 0.5 μm thick), and from 0.2 to 0.6 for nanocomposite films (25 ± 0.5 μm thick). (where p is the experimental pressure and p_0 is the saturation pressure of water vapour at 30 °C, corresponding to 31.8 Torr) The experiments with ammonia vapour were performed at 30 °C and at relative pressures equal to 0.0115 and 0.0883. These relative pressures correspond to ammonia pressures of 100 and 770 Torr (in this case p_0 at 30 °C is equal to 8722.2 Torr [28]). Film thickness was 15 ± 0.5 μm for the polyimide and 25 ± 0.5 μm for the silica hybrid. For experiments with water vapour the relative pressure has been assumed to be equal to the water activity, in view of the low value of p_0. For the latter case, water activity, a, is defined as the ratio of the fugacity of the vapour at the test condition and the fugacity of the vapour in a reference state. Therefore, if we take as a reference state the water vapour at saturation condition and assume that in this condition the behaviour of the vapour is equivalent to that of an ideal gas, then $a = p/p_0$.

2.2.2. Gravimetric analysis

The equipment used to determine the weight gain of samples exposed to a controlled humidity environment is similar to that used for the on-line FTIR spectroscopy measurements. In place of the FTIR measuring cell an electronic microbalance Model D200 by CAHN Instrument was used. This has an accuracy of 0.1 μg.

2.3. FTIR data analysis

2.3.1. Water sorption

Whenever required, the absorbance spectra of both dry films and films containing the penetrant, were obtained from the single beam spectra using the cell without film as background. These spectra are reported in Fig. 2a for the polyimide and in Fig. 2b for the corresponding silica-nanocomposite. An inspection of Fig. 2a and b shows that the sorbed water brings about an increase in absorbance in the ν_{OH} range (around 3400 cm^{-1}) and in the in-plane bending interval (around 1600 cm^{-1}). The spectra of sorbed water at different times were isolated by eliminating the interference caused by the polymer matrix. This was accomplished by using the ratio method [29], by which the absorbance spectrum at time t is calculated, using the single beam spectrum of the dry specimen as background, i.e.

$$A_t(\nu) = \log \frac{I_0(\nu)}{I_t(\nu)} \tag{1}$$

where $A_t(\nu)$ is the absorbance spectrum of the penetrant, $I_0(\nu)$ is the single beam spectrum collected at time = 0 (dry specimen) and $I_t(\nu)$ is the single beam spectrum at time t. It is noted that $A_t(\nu)$ corresponds to the subtraction spectrum $A_d(\nu)$:

$$A_d(\nu) = A_t(\nu) - K \times A_0(\nu) \tag{2}$$

where K is the subtraction factor, i.e. an adjustable parameter used to compensate for possible thickness

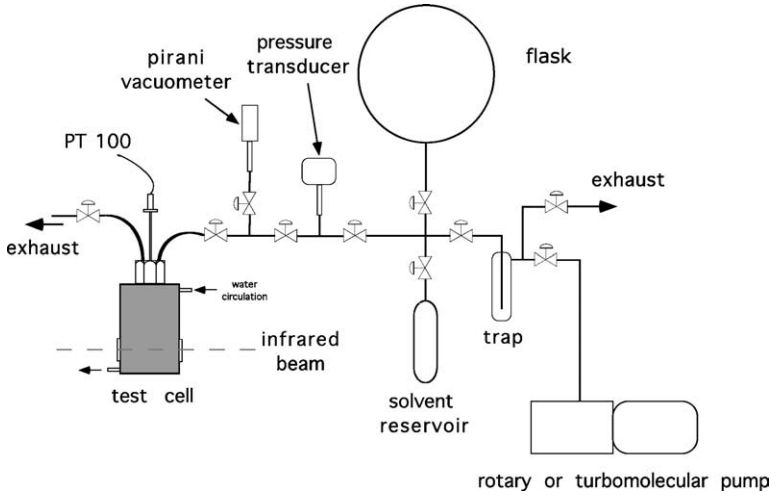

Fig. 1. Schematic representation of the experimental apparatus for sorption–desorption tests by time-resolved FTIR spectroscopy.

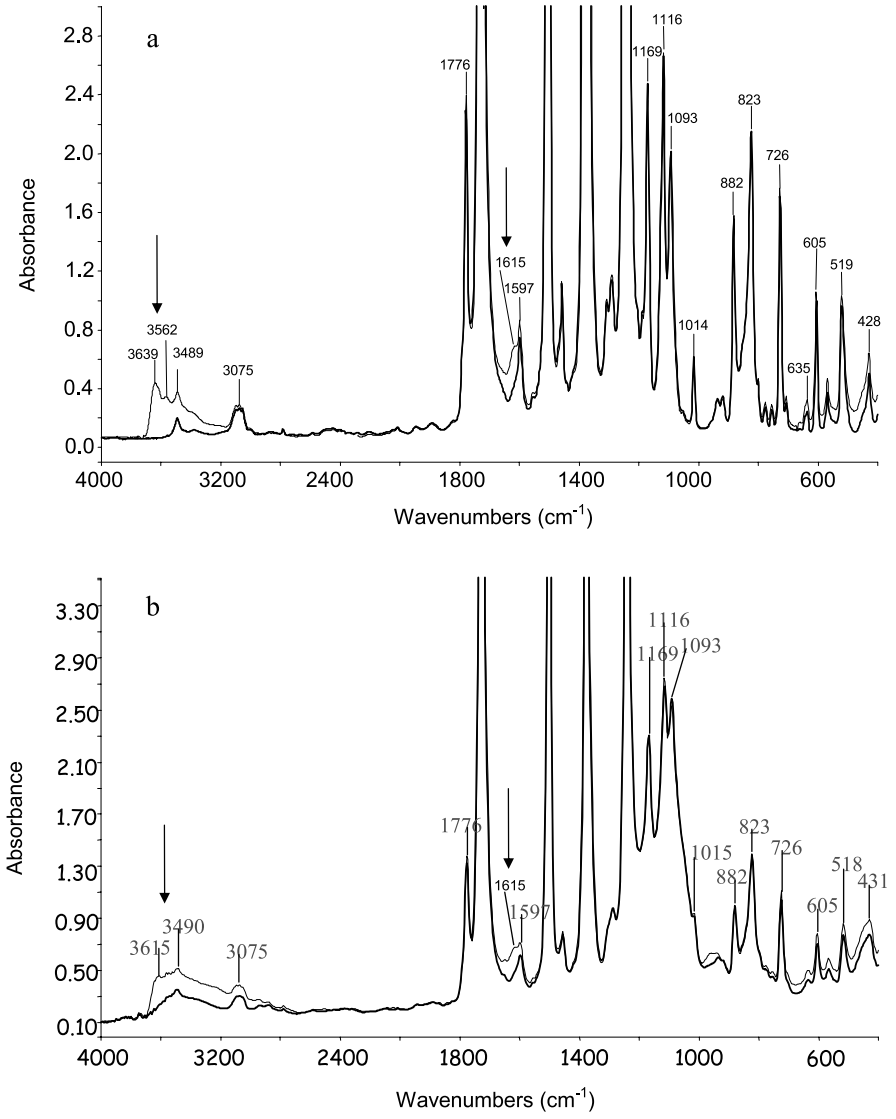

Fig. 2. Absorbance spectra in the 4000–400 cm^{-1} range for dry samples (thick line) and for samples equilibrated at water vapour activity = 0.4 (thin line): (a) pure polyimide; (b) silica hybrid.

differences between 'wet' and 'dry' samples. The above equation holds for conditions in which K is equal to 1, that is to say when there is a negligible change in volume as a result of penetrant sorption, as it is the case for the present systems. When this condition is satisfied Eq. (1) can be used in place of the more general Eq. (2). Moreover, the use of Eq. (1) is generally preferred as it avoids the problems related to the long-term background instability. The absorbance areas of the subtraction spectra in the ν_{OH} region (3800–3000 cm^{-1}) and in the in-plane bending interval (1680–1570 cm^{-1}) were used to monitor the amount of water present in the sample as a function of time [$A(t)$].

For the case of unresolved, multicomponent bands, a curve resolving algorithm based on the Levenberg–Marquardt method was used to separate the individual peaks [30]. In order to reduce the number of adjustable parameters, both the baseline, the band shape and the number of components were fixed and the curve-fitting program was used to calculate the height, the full width at half height (FWHH) and the position of the individual components. The minimum number of components was determined by visual inspection and by a second- derivative analysis of the experimental profile. The peak function used throughout was a mixed Gaussian–Lorentzian line-shape [31].

2.3.2. Ammonia sorption analysis

The data treatment for the sorption of ammonia was analogous to that previously described for water sorption. The evolution of the IR spectrum of polyimide was also monitored to gather information on the progress of the chemical reaction occurring between ammonia and imide groups. The wavenumber range used to monitor the sorption

of ammonia in polyimide was 3500–3200 cm^{-1}, while the chemical reactions were followed by observations in the peaks at 1778, 1377, 1169 and 726 cm^{-1}.

With the lowest relative pressure ($p/p_0 = 0.0115$, i.e. $p =$ 100 Torr) for samples 15 μm thick, the characteristic time of diffusion is much shorter than that for the chemical reaction and, therefore, it makes it possible to decouple the two processes. At the higher relative pressure ($p/p_0 = 0.0883$, i.e. $p = 770$ Torr) the large increase in reaction rate prevents a separate analysis of the two phenomena to be carried out. This issue will be discussed in more detail later.

In the case of the nanocomposite, the ammonia sorption kinetics could not be determined due to the superposition of diffusion and reaction processes. This is attributed to the much higher reaction rate in the presence of the inorganic phase, and to a characteristic diffusion time longer than for the case of pure polyimide, owing to the larger thickness of the hybrid samples. In this latter case, only the evolution of the polyimide component was followed, at the same frequencies selected for pure polyimide.

3. Results and discussion

3.1. Sorption of water in polyimide and nanocomposite

In Figs. 3 and 4 are reported the water spectra in the ν_{OH} stretching region collected at sorption equilibrium ($a = 0.4$) for the polyimide and the nanocomposite films. The complex spectral profiles were resolved by a curve fitting analysis. The resulting components are reported on the same figures.

The three component spectrum of water dissolved in pure polyimide can be interpreted in terms of a simplified association model, whereby three different water species (S_0, S_1 and S_2) can be spectroscopically distinguished, on the basis of the strength and the number of H-bonding

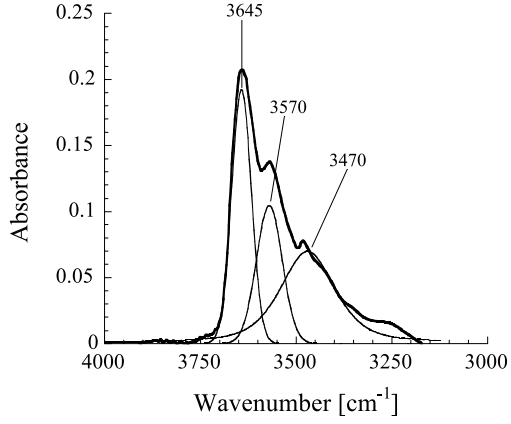

Fig. 3. Curve fitting analysis of the spectrum representative of water sorbed at equilibrium ($a = 0.4$) in neat polyimide. The figure displays the resolved components (thin lines) and the experimental profile (thick line).

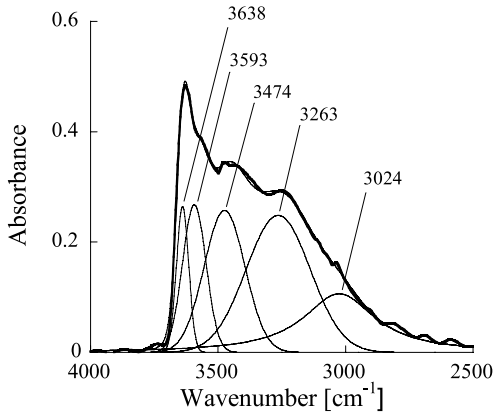

Fig. 4. Curve fitting analysis of the spectrum representative of water sorbed at equilibrium ($a = 0.4$) in the polyimide-silica hybrid sample. The figure displays both the resolved components (thin lines) and the experimental profile (thick line).

interactions that they form with proton accepting groups [27,32,33].

In particular, the peak at higher frequency (3645 cm^{-1}) corresponds to those water molecules in which the hydrogens do not form any interaction of the H-bonding type (S_0). This is not to say that these water species are to be regarded as completely detached from the surrounding polymer chains. Weaker polymer-penetrant interactions (dipole–dipole, charge transfer), which are undetectable by vibrational spectroscopy measurements in the ν_{OH} region, may still exist. Therefore, the term 'free' water, often used to describe these species, has to be interpreted as 'free' from H-bonding association as proton donors.

The partially resolved component at 3570 cm^{-1} arises from water molecules forming a single H-bonding interaction with proton acceptor groups (S_1). In pure polyimide, in addition to the imide carbonyls, (which have been shown to posses a reduced tendency to act as proton acceptors [34]), there are also the ether oxygens within the ODA units that are capable of playing this role. It should be noted, however, that self-associated water dimers are expected to absorb at the same frequency. At present there is insufficient spectroscopic evidence for the relative validity of the two hypotheses; further vibrational spectroscopy measurements are in progress to clarify the nature of the species absorbing at 3570 cm^{-1}.

The broad component centred at 3470 cm^{-1} originates from water species having both hydrogens involved in H-bonding (S_2). Once again, these species may correspond to single penetrant molecules bridged to two adjacent proton acceptors in the polyimide chains (ether oxygens) or to self-associated water in molecular clusters. In view of the low interactive character of the PMDA-ODA polyimide [34,35] and because of the severe geometrical constraints associated with the formation of such polymer/penetrant complexes the occurrence of water clustering is a more feasible explanation.

In comparing the spectra of water dissolved in the pure

polyimide with that in the nanocomposite films (Figs. 3 and 4), significant differences emerge in terms of number of interacting species and their population. The observation that in the spectrum of Fig. 3 there is only one S_2 component, while in Fig. 4 can be identified at least three distinct peaks, points to the presence of a single S_2 adduct in the pure polyimide film and to a series of H-bonding complexes in the polyimide/silica nanocomposite, which are characterised by different interaction strengths (i.e. the lower the frequency of the component, the higher the strength of the H-bond).

The normalised absorbance of the ν_{OH} water band is considerably higher in the nanocomposite than in pure polyimide, suggesting that there is a higher amount of sorbed water in the system. At the same time, there is a considerably higher contribution to H-bonding from strongly interacting species. This can be explained on the basis that the silica domains in the nanocomposite system contain a large amount of surface OH groups, which promote strong H-bonding interactions. The relative contributions (at sorption equilibrium) of the different water species, evaluated by curve fitting analysis, are reported as a function of the water vapour activity in Fig. 5 for the polyimide and in Fig. 6 for the nanocomposite. In the latter case the relative contributions of S_0, S_1 and S_2 species are slightly dependent of water activity. Conversely, significant changes are observed for pure polyimide. In both cases, however, the relative concentration of S_2 species increases with total concentration of absorbed water. For the case of pure polyimide this effect may be related to the tendency of water to form clusters, which increases with increasing the amount absorbed in the film [36–40]. On the other hand, for the case of the nanocomposite this is likely to be due to the fact that, at the levels of water activity used in the experiments, the adsorption of water molecules on the interacting sites of the inorganic phase is far from the saturation conditions. In terms of absorbance areas, the S_2 species within the nanocomposite have a higher absorbance (by almost one order of magnitude), than those of S_0 and S_1,

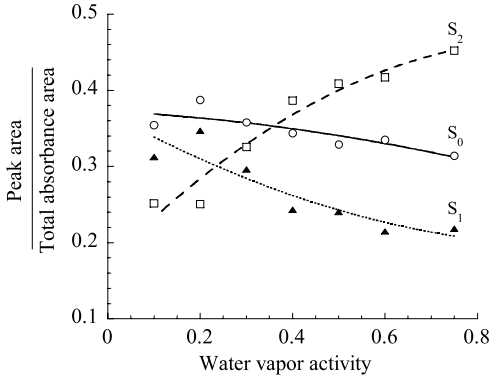

Fig. 5. Plots of the ratio of area of the individual component peaks to the total absorbance area, for the water spectra collected at vapour sorption equilibrium, against water vapour activity. Data for the tests performed on the neat polyimide at 30 °C. Lines are drawn to guide the eye.

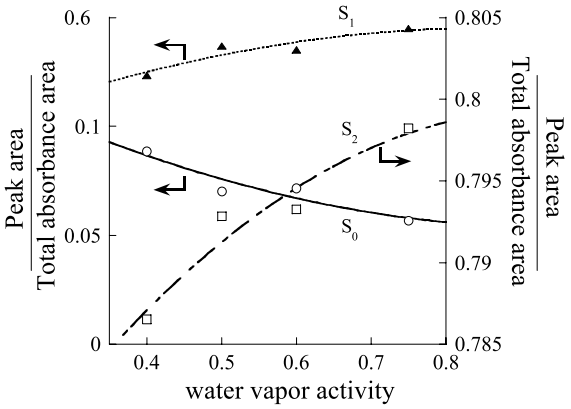

Fig. 6. Plots of the ratio of area of the individual component peaks and the total absorbance area, for the water spectra collected at vapour sorption equilibrium, against water vapour activity. Data for the tests performed on the hybrid sample at 30 °C. Lines are drawn to guide the eye.

whereas for pure polyimide comparable values of the relative absorbance areas are found. This confirms the much stronger interactive character of the hybrid system, resulting from the presence of the inorganic domains.

Sorption isotherms evaluated gravimetrically, reported in Fig. 7, are consistent with this interpretation, not only because the solubility of water in the hybrid is higher but also in view of the significant difference in the shape of the isotherms. In the case of polyimide the upward concavity at higher activities can be related to the occurrence of water clustering which contributes to an increase in water solubility with increasing water activity [37–40]. The slight downward concavity of the isotherm in the case of the nanocomposite, on the other hand, points to the presence of water adsorbed on specific sites within the inorganic phase. No upturn is evident in this case, owing to the increased hydrophilicity of the substrate, which prevents the occurrence of water clustering.

Fig. 8 shows the time-resolved FTIR spectra of sorbed water, in two wavenumber ranges of interest, collected at several time intervals for experiments on a pure polyimide sample at $a=0.4$. In particular, the spectra in the 1690–

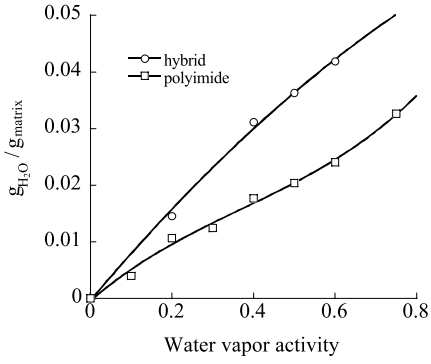

Fig. 7. Sorption isotherms at 30 °C expressed as plots of mass of sorbed water per unit mass of absorbate against water vapour activity for neat polyimide (open squares) and corresponding hybrid sample (open circles).

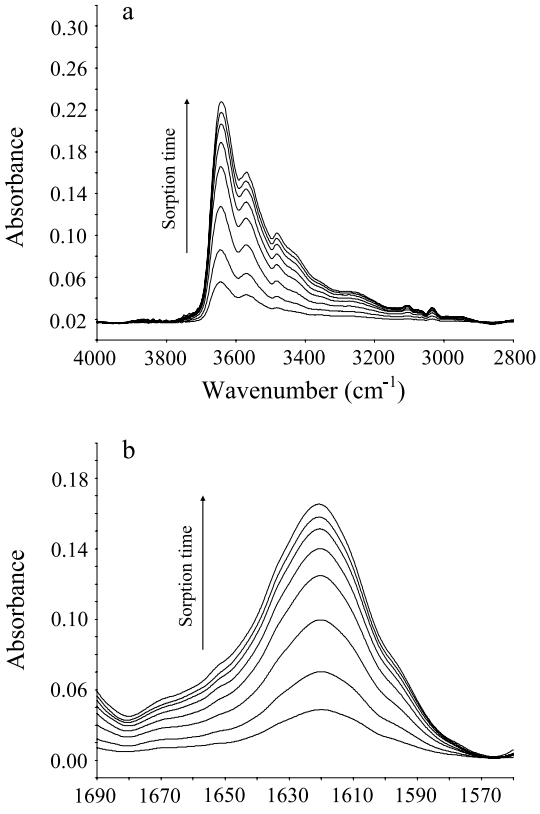

Fig. 8. FTIR transmission spectra collected at different time intervals during the sorption experiment of water in neat polyimide ($a=0.4$, $T=30$ °C). Collection time increases as indicated by the arrow. (a) 4000–2800 cm^{-1} interval; (b) 1690–1560 cm^{-1} interval.

1560 cm^{-1} range (shown in Fig. 8b), displays the H_2O bending mode in the form of a well resolved signal. These were used to calculate the relative concentration of the different water species, taking into account the band area in the ν_{OH} interval. The existence of two distinct absorption frequency bands illustrate other features of the diffusion behaviour of the two systems. In this respect, it is noted that the molar absorptivity of the stretching modes, ε_ν, is far more sensitive to molecular interactions than that of the bending vibrations, ε_δ. As a result of H-bonding formation the ε_ν values can increase by one order of magnitude, while the ε_δ values remain nearly constant [39,40]. Thus, if the relative population of interacting and non-interacting species changes during the sorption stage, the absorbance ratio between the stretching and the bending bands will also change, causing a detectable deviation from linearity in an the absorbance/absorbance plots.

Examples of sorption/desorption kinetics evaluated from the absorbance area of the stretching band of water are reported in Fig. 9a for the polyimide and in Fig. 9b for the nanocomposite. Exactly the same results (data not shown) were obtained from the analysis of the δ_{HOH} band. For both materials the desorption kinetics is always slower than the preceding sorption, which is a typical feature of Fickian systems when the mutual diffusivity is an increasing

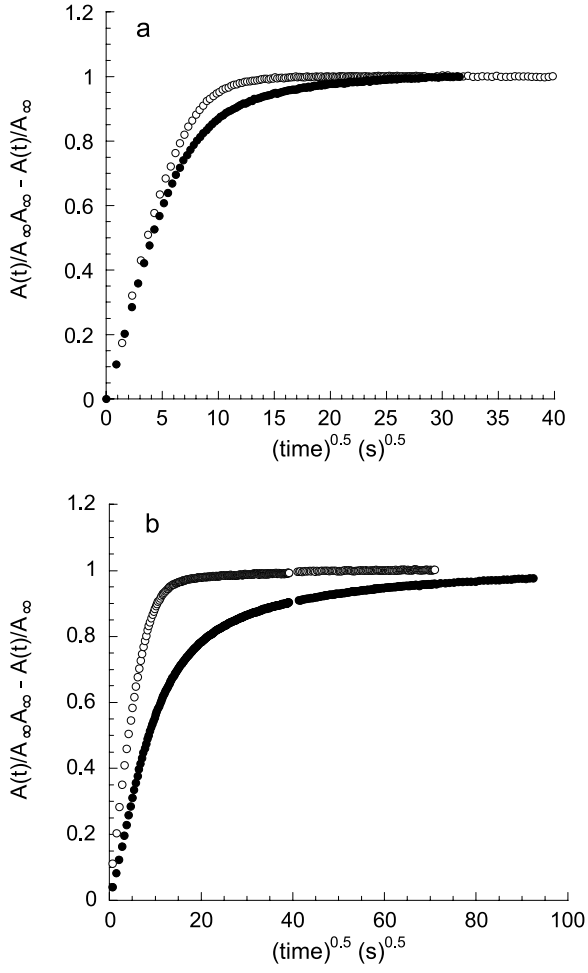

Fig. 9. Comparison between sorption and desorption kinetics at $a=0.4$ evaluated spectroscopically from the absorbance area of the water band in the 3800–3000 cm^{-1} interval. (a) pure polyimide; (b) silica hybrid sample.

function of penetrant concentration [41]. This effect is more pronounced in the case of the polyimide-silica hybrid sample, due to the strong interaction of water molecules with the inorganic phase which slows down the desorption process. When the diffusivity increases with concentration, the shape of the sorption curve does not depend significantly on the functional form of the diffusion coefficient. Sorption kinetics can be adequately described in this case, using an effective constant diffusivity (D), by the following relationship for a one-dimensional geometry [42]:

$$\frac{M_t}{M_\infty} = 1 - \frac{8}{\pi^2}\sum_{m=0}^{\infty}\frac{1}{(2m+1)^2}\exp\left[\frac{-D(2m+1)^2\pi^2 t}{L^2}\right] \quad (3)$$

In this equation M_t is the amount of penetrant absorbed at time t, M_∞ is the amount of penetrant absorbed at equilibrium, L is the thickness of the film, and m is an integer.

Eq. (3) has been used to fit the sorption data. The D parameter determined from the fitting process is reported in Fig. 10, as a function of average water concentration. This

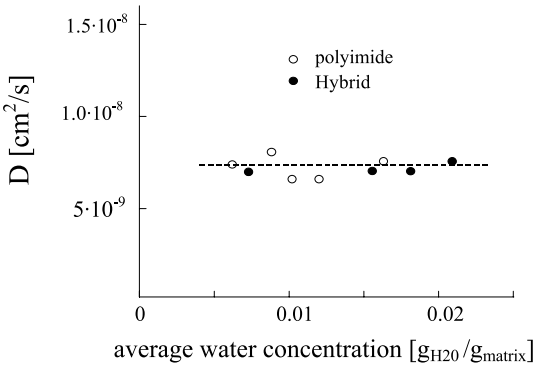

Fig. 10. Water diffusivity at 30 °C vs. average water concentration for neat polyimide (open circles) and silica hybrid sample (closed circles).

shows that the diffusivity is very similar for both materials. It is worth noting that D represents an average diffusivity within the range of water concentration present in the sample during the sorption experiment. Although a comparison of sorption and desorption kinetics points to a dependence of D on water concentration, the actual averaged values do not show such a dependence.

It should be pointed out, however, that the analysis used here provides only a limited insight in the mass transport of penetrants in heterogeneous systems, such as the nanocomposites of the present study. The diffusion kinetics for these systems are rather complex due to structural and interactional peculiarities.

In Fig. 11 are reported the normalised absorbance values of the ν_{OH} water band, measured at different time intervals during the sorption experiments, against the corresponding absorbance values of the δ_{HOH} water band. In the case of the polyimide (Fig. 11a) the data deviate significantly from the expected linear behaviour, in the form of an upward concavity. The upper concavity of the curves in Fig. 11b indicate that the contribution of the low frequency components of the stretching band (interacting species) becomes increasingly more significant with increasing the water concentration in the sample. This is consistent with the water clustering behaviour, which is expected to depend on the total water content in the same manner. Conversely, for the nanocomposite sample (Fig. 11b) the data gathered at the different water activities can all be accommodated on a linear 'master curve'. A slight upturn is observed only towards the upper end of the absorbance interval (i.e. at the highest concentration of sorbed water). This behaviour points to a constant ratio between the concentration of the different water species, which is attained instantaneously. This is likely to be due to the fact that in the nanocomposite the prevailing water species are those interacting with the inorganic component, since the main sorption mechanism is the adsorption at specific interaction sites within the inorganic phase. Consequently the adsorption behaviour monitored by spectroscopic analysis is essentially that of S_2 species.

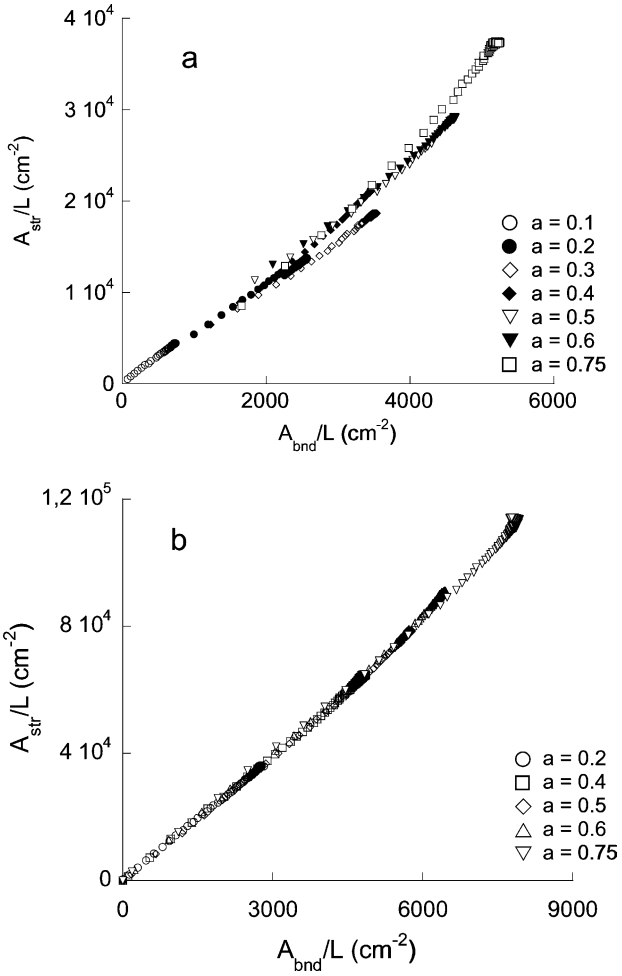

Fig. 11. Figures 11 Reduced absorbance (A/L) of the ν_{OH} water band as a function of the reduced absorbance of the δ_{HOH} water band for sorption experiments performed at the different activities. (a) pure polyimide; (b) silica hybrid sample.

3.2. Sorption of ammonia in polyimide and nanocomposite films

The time evolution of the sample spectrum in the 3470–3000 cm^{-1} frequency range is reported in Fig. 12 with reference to sorption experiments conducted on the polyimide film at 100 Torr and 30 °C. The diffusing ammonia is clearly detectable by the presence of two well resolved peaks at 3400 and 3306 cm^{-1} assigned, respectively, to the asymmetric and symmetric stretching modes of NH_3. A gradual increase in absorbance over the whole 3470–3000 cm^{-1} range, observed in the same time frame, is due to a concurrent reaction of ammonia with the imide groups in the polymer. After a short time (about 5 min) the intensity of both ammonia peaks reaches the sorption equilibrium conditions.

At longer times, the whole spectrum of the polyimide displays dramatic changes, as a result of the reactions taking place between penetrant and absorbant. An example of these events is shown in Fig. 13, where are compared the spectra

collected at 0.14 and 28 h in the range 2000–1000 cm^{-1} for the sorption experiment conducted on the polyimide film at 100 Torr and 30 °C. These show the extensive reduction of intensity for the peaks attributed to the imide groups at 1778, 1725, 1377 and 1170 cm^{-1}, and the concurrent increase of absorptions at 1670, 1606 and 1408 cm^{-1}. The latter can be attributed to the normal modes of the amide groups, formed as the products of the reaction, according to the following scheme:

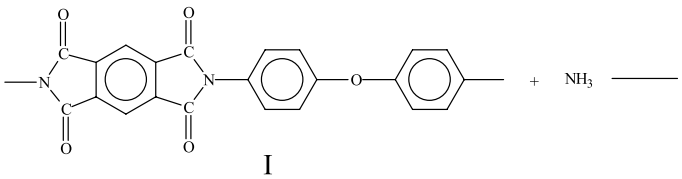

I II

These experimental findings demonstrate that the diffusion and reaction processes are well separated in time (sequentially). This makes it possible to determine the relative mass transport parameters.

The evolution of the peaks at 3400 and 3306 cm^{-1} with time, in terms of normalised absorbance (i.e. $A(t)/A_\infty$, with A(t) absorbance at time t and A_∞ absorbance at sorption equilibrium) is reported in Fig. 14. The analysis of sorption kinetics, assuming ideal Fickian behaviour [41], gave a calculated ammonia diffusivity value equal to 2.2×10^{-9} cm^2/s (see later).

Differential mass balances were used to better illustrate aspects of the coupled diffusion-reaction of ammonia. The evolution of the reacting species was modelled by means of differential mass balance equations. Since the penetrant is the only mobile component of the system, the following schematic approach can be used to illustrate the relevant features of time evolution of ammonia (referred to as component A) and of imide moiety (referred to as component B). The differential mass balances of species A and B are one-dimensional and can be described by the equations:

$$\frac{\partial C_A}{\partial t} = D\frac{\partial^2 C_A}{\partial x^2} - kC_A C_B \tag{4}$$

$$\frac{\partial C_B}{\partial t} = -kC_A C_B \tag{5}$$

In Eqs. (4) and (5), it is assumed that an irreversible bimolecular reaction takes place according to the simple scheme:

$$A + B \rightarrow C$$

Here D is the mutual diffusivity of species A in the matrix and k is the reaction kinetic constant. C_i is the concentration of species 'i', t is the time and x is the spatial coordinate normal to the sheet surface.

These balances are coupled with appropriate boundary and initial conditions, which for thin sheets become:

$$\left.\begin{aligned} C_B &= C_{B0}; \quad \forall x, t = 0 \\ C_A &= 0; \quad \forall x, t = 0 \end{aligned}\right\} \text{Initial conditions}$$

$$C_A = C_{A0}; \quad \forall t, x = 0, L \text{ Boundary conditions}$$

In order to separate the relative contribution of the diffusive and reactive terms, it is useful to write the mass balances in dimensionless form:

$$\frac{\partial C_A^*}{\partial t^*} = \frac{\partial^2 C_A^*}{\partial x^*} - \alpha' C_A^* C_B^* \tag{4'}$$

$$\frac{\partial C_B^*}{\partial t^*} = -\alpha'' C_A^* C_B^* \tag{5'}$$

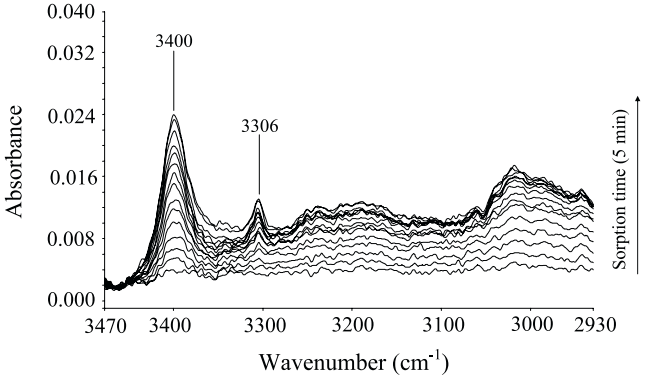

Fig. 12. FTIR transmission spectra in the 3470–3000 cm^{-1} range collected at different time intervals during the sorption experiment of ammonia in neat polyimide. (p_{NH_3} = 100 Torr; T = 30 °C). The figure reports the spectra collected in the first 5 min. Collection time increases as indicated by the arrow.

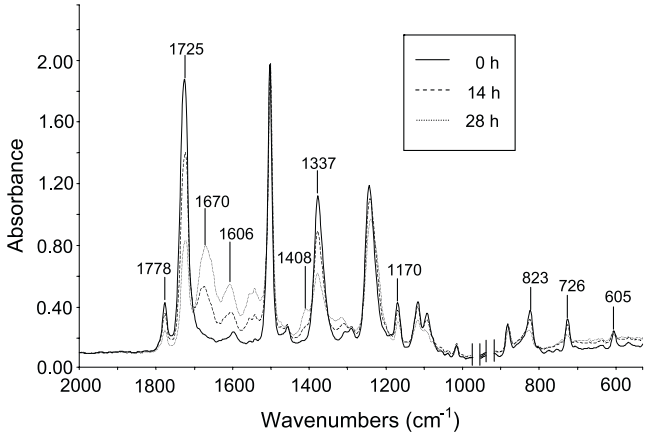

Fig. 13. FTIR transmission spectra in the 2000–600 cm^{-1} range, collected at three times (0, 14 and 28 h) during the sorption of ammonia in neat polyimide (p_{NH_3} = 100 Torr; T = 30 °C).

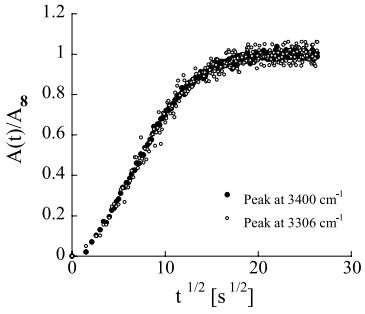

Fig. 14. $A(t)/A_\infty$ for the sorption test of ammonia in neat polyimide ($p_{NH_3} = 100$ Torr; $T = 30$ °C).

where

$$C_A^* = C_A/C_{A0};\ C_B^* = C_B/C_{B0};\ x^* = x/L;\ t^* = \frac{tD}{L^2}$$

$$\alpha' = \tau_D/\tau'_R;\ \alpha'' = \tau_D/\tau''_R \quad \tau_D = L^2/D \quad \tau'_R = (kC_{B_0})^{-1};$$

$$\tau''_R = (kC_{A_0})^{-1}$$

Thus, three characteristic times can be defined: τ_D, representing the diffusive characteristic time and τ'_R and τ''_R, are chemical reaction characteristic times.

If the diffusive characteristic time, τ_D, is much smaller than both τ'_R and τ''_R, then for sorption times smaller than or equal to τ_D,α' and α'' become very small and the mass balance equations reduce to a purely diffusional process of species A.

In the present case (i.e. for $T = 30$ °C, $p = 100$ Torr, and $L = 15$ μm), the value τ_D, estimated to be in the region of 250 s, is much smaller than τ_R, which is of the order of several hours (Fig. 13). The diffusion and reaction processes, being well separated in time, enables the analysis of the sorption process to be made independently of the occurrence of any reaction, and makes it possible to calculate the value for ammonia diffusivity (reported earlier). Results of a gravimetric analysis of the diffusion of ammonia in Kapton® polyimide films at 30 °C have been already reported by Iler et al. [26,42] for the same experimental conditions used in the present study. The sorption kinetics curves were interpreted using an approach proposed by Danckwerts [43] for the case of diffusion-reaction processes with a pseudo-first order reaction. These authors have calculated diffusivity values for ammonia which were at least two order of magnitude lower than those expected on the basis of simple size related factors (Fig. 15). In this figure is shown a plot of the diffusion coefficient at infinite dilution for various penetrant relative to the polyimide film at 30 °C using the van der Waals volume, b, of the penetrant as correlating parameter [16]. Iler et al. have attributed this deviation to strong interactions occurring between ammonia and polyimide which impose a large activation energy for the diffusional 'jump' to take place. The value obtained in this study (using time resolved FTIR spectroscopy) on the other hand, is quite close to the value expected on the basis of the molecular size of the penetrant. The slight positive deviation can be reasonably attributed to the increase of diffusivity with penetrant concentration and to the fact that PMDA-ODA samples prepared for this study are somewhat different with respect to the molecular configuration/orientation of commercial polyimide (Kapton®) used by previous workers. The findings of this study, therefore, rule out the hypothesis proposed by Iler et al. [16,42] that the penetrant mobility is hindered by strong polymer/penetrant interactions.

The same analysis used for the diffusion of ammonia in polyimide at $p = 100$ Torr cannot be used for the experiment carried out at 770 Torr, owing to the occurrence of much faster reactions, which do not allow to separate the diffusion and reaction processes.

It should be noted that if there is no interference between the spectroscopic signals deriving from the reaction with the signals from the diffusing molecule, the possibility to monitor concurrently the events in both processes is not restricted to cases where there are well separated characteristic times for the two processes. In such cases, information gathered from time resolved FTIR spectroscopy can be analysed using the complete form of Eq. (4) and (5), and can be used to monitor the diffusion-reaction process, even though the two phenomena are coupled.

The kinetics of the chemical reaction with time can be followed by monitoring the absorbance of several peaks related to the imide groups. In the present study the peak centered at 726 cm^{-1} was used for this purpose, since it is well resolved both for the pure polyimide and the corresponding silica-hybrid. The behaviour of the two materials is compared in Fig. 16 at 770 and 100 Torr. The reactivity of the polyimide, under these conditions, is clearly evident and results in a final conversion of imide rings greater than 60% at the highest pressure (770 Torr).

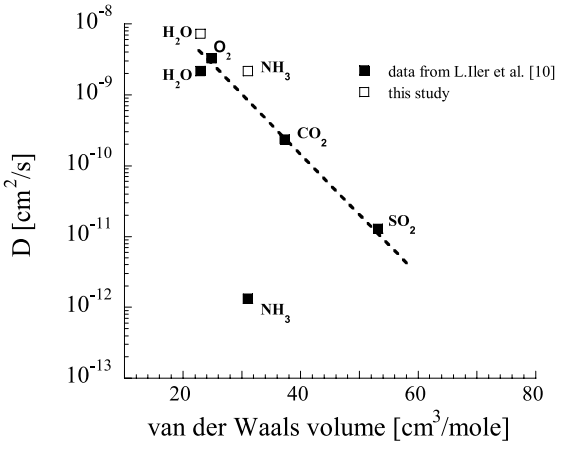

Fig. 15. Correlation of diffusion coefficient at infinite dilution for various penetrants in Kapton® at 30 °C with van der Waals volume, b, of the penetrant. Closed squares refer to data from Iler et al. [10], open squares refer to ammonia ($p_{NH_3} = 100$ Torr) and water diffusivities evaluated in the present study.

The reaction rate is considerably faster in the case of the corresponding silica-hybrid films.

A possible explanation for this effect is that the hydroxyl groups within the silica phase, form H-bonding interactions with the carbonyl groups of the imide ring, reducing the electron density on the carbon atom, which facilitates the nucleophilic attack of the ammonia. Another reason can be the increased concentration of sorbed ammonia in the nanocomposite, due to the strong interactions of ammonia with the surface OH groups of the silica domains. The resulting confinement of the ammonia would also provide the conditions for faster reactions at the interface, which are very significant owing to the large surface area of the silica domains in hybrid systems. Gravimetric measurements of ammonia diffusion are in progress to elucidate this point.

Owing to the insolubility of polyimides in conventional solvents it is not possible to determine whether concurrent chain scission reactions have taken place.

It is expected, however, that ring opening of the imide groups would occur at a much faster rate than the hydrolysis of the amide groups in the polyamic acid, particularly under basic conditions. However, in view of the very high conversion levels observed for the opening of the imide rings, the possibility of degradation reactions extending to chain scission cannot be ruled out.

4. Conclusions

(a) For the diffusion of water through polyimide films, the FTIR spectroscopic analysis has demonstrated that the prevailing penetrant species is monomeric water along with a minor contribution from self-associated species (dimers and multimers). In the polyimide-silica hybrids the amount of H-bonded water increases substantially as a result of molecular interaction occurring with the inorganic domains. However, the diffusion behaviour is Fickian, and substantially linear for both materials, in so far as the diffusivity is independent of concentration.

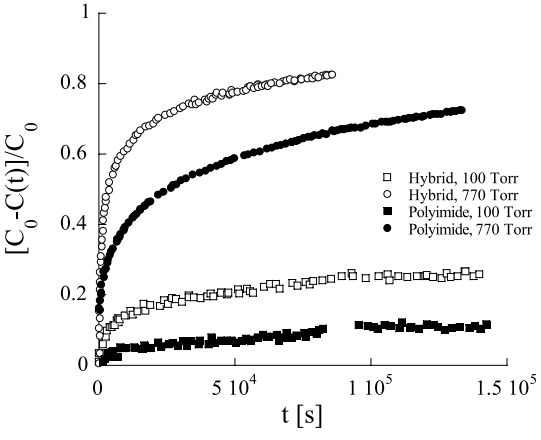

Fig. 16. Relative conversion of the imide groups at 30 °C as a function of time for both neat polyimide and silica hybrid sample.

(b) Extensive reactions take place between the ammonia penetrant and the sorbated polyimide. Morever, the chosen experimental conditions, have made it possible to estimate the relative characteristic times for the two consecutive processes, physical diffusion and reaction of ammonia.

(c) The imide ring opening reactions caused by ammonia are considerably faster for the case of polyimide-silica hybrids due to the confinement effect imposed by the nanostructured silica domains. This widens the possibility of utilising organic–inorganic hybrids for other catalytic processes involving reactions with reactive penetrants.

References

[1] Ghosh MK, Mittal KL, editors. Polyimides: fundamentals and applications. New York: Marcel Dekker; 1996.
[2] Bessonov MI, Zubkov VA. Polyamic acids and polyimides: synthesis, transformation and structure. Boca Raton, FL: CRC Press; 1993.
[3] Thompson LF, Wilson CG, Tagawa S, editors. Polymers for microelectronics: resists and dielectrics. ACS symposium series, 537. Washington DC: ACS; 1994.
[4] Yang YK, Koros WJ, Hopfenberg HB, Stannet VT. J Appl Polym Sci 1986;31:1619.
[5] Hofman D, Ulbrich J, Fritsch D, Paul D. Polymer 1996;37:4773.
[6] Morikawa A, Iyoku Y, Kakimoto M, Imal Y. Polym J 1992;24:107.
[7] Kioul A, Mascia L. J Non-Cryst Solids 1994;175:169.
[8] Wang S, Hamad Z, Mark JE. Chem Mater 1994;6:643.
[9] Mascia L. Trends Polym Sci 1995;3:61.
[10] Nandi M, Conklin JA, Salvati Jr L, Sen A. Chem Mater 1991;3:201.
[11] Strawbridge I. In: Paul A, editor. Chemistry of glasses. Chapman and Hall; 1990.
[12] Huang H, Glaser RH, Wilkes GL. In: Zeldin M, Winne KJ, Allcock HR, editors. Inorganic and organometallic polymers. ACS symposium series, 360. Washington DC: ACS; 1987.
[13] Brinker CJ, Scherer GW. Sol-gel science: the physics and chemistry of sol-gel processing. London: Academic press; 1990.
[14] Klein LC, Garvey GL. In: Brinker CJ, Clark DJ, Ulrich DR, editors. Better ceramics through chemistry. Mat res soc symp proc, vol. 32. Pennsylvania: Elsevier; 1984. p. 3339.
[15] Rabinowich EM. Sol-gel optics: processing and applications. USA: L.C. Kluwer, Academic Publishers; 1994. pp. 1–37.
[16] Musto P, Ragosta G, Scarinzi G, Mascia L. Polymer 2004;45:1697.
[17] Schrotter JC, Smaihi M, Guizard G. J Appl Polym Sci 1966;61:2137.
[18] Mascia L, Kioul A. Polymer 1995;36:3649.
[19] Yen C-T, Chen W-C, Liaw D-J, Lu H-S. Polymer 2003;44:7079.
[20] Karpova IL, Dragan KS, Privalko EG, Privalko VP. Sci Technol Adv Mater 2003;4:115.
[21] Li C-F, Zhong S-H. Catal Today 2003;82:83.
[22] Cornelius CJ, Marand E. J Membr Sci 2002;202:97.
[23] Hibshman C, Mager M, Marand J. Membr Sci 2004;229:73.
[24] Musto P, Ragosta G, Mascia L. Chem Mater 2000;12:1331.
[25] Musto P, Ragosta G, Scarinzi G, Mascia L. J Polym Sci, Part B: Polym Phys 2002;40:922.
[26] Iler L, Koros WJ, Yang DK, Yui R. In: Mittal KL, editor. Polyimides. synthesis, characterization and applications, 1. New York: Plenum Press; 1984. p. 443.
[27] Cotugno S, Larobina D, Mensitieri G, Musto P, Ragosta G. Polymer 2001;42:6431.
[28] Perry RH, Green DW, Maloney JO, editors. Perry's chemical engineers handbook. 7th ed. New York: McGraw Hill; 1999.

[29] Koenig JL. Adv Polym Sci 1984;52:87.
[30] Marquardt DW. J Soc Ind Appl Math 1963;11:441.
[31] Maddams WF. Appl Spectrosc 1980;34:245.
[32] Musto P, Karasz FE, MacKnight WJ. Polymer 1989;30:1012.
[33] Mensitieri G, Cotugno S, Musto P, Ragosta G, Nicolais L. In: Mittal KL, editor. Polyimides and other high temperature polymers: synthesis. Characterization and applications, vol. 2. The Netherlands: VSP Publ; 2003.
[34] Zimm BH. J Chem Phys 1953;21:934.
[35] Zimm BH, Lundberg JL. J Phys Chem 1956;60:425.
[36] Lundberg JL. J Macromol Sci B 1969;3:693.
[37] Lundberg JL. J Pure Appl Chem 1972;31:261.
[38] Starkweather Jr HW. Polym Lett 1963;1:133.
[39] Pimentel GC, McClellan AL. The hydrogen bond. San Francisco, USA: W.H. Freeman and Co.; 1960.
[40] Murthy ASN, Rao CNR. Appl Spectrosc Rev 1968;2(1):69.
[41] Crank J. The mathematics of diffusion. 2nd ed. Oxford: Clarendon Press; 1975.
[42] Iler LR, Laundon RC, Koros WJ. J Appl Polym Sci 1982;27:1163.
[43] Danckwerts PV. Trans Farad Soc 1951;47:1014.